



Two New $\text{Ag}^{\text{I}}/\text{Mn}^{\text{II}}$ Complexes with Two/Three-Dimensional Supramolecular Structures Based on the [2-(4'-pyridyl)-benzoxazole] Ligand

Qizhong Lin, Jianteng Wang, Yicheng Zhang, Li Song & Wenxiang Chai

To cite this article: Qizhong Lin, Jianteng Wang, Yicheng Zhang, Li Song & Wenxiang Chai (2015) Two New $\text{Ag}^{\text{I}}/\text{Mn}^{\text{II}}$ Complexes with Two/Three-Dimensional Supramolecular Structures Based on the [2-(4'-pyridyl)-benzoxazole] Ligand, Molecular Crystals and Liquid Crystals, 623:1, 234-244, DOI: [10.1080/15421406.2015.1010920](https://doi.org/10.1080/15421406.2015.1010920)

To link to this article: <http://dx.doi.org/10.1080/15421406.2015.1010920>



Published online: 21 Dec 2015.



Submit your article to this journal [↗](#)



Article views: 5



View related articles [↗](#)



View Crossmark data [↗](#)

Two New Ag^I/Mn^{II} Complexes with Two/Three-Dimensional Supramolecular Structures Based on the [2-(4'-pyridyl)-benzoxazole] Ligand

QIZHONG LIN,¹ JIANTENG WANG,² YICHENG ZHANG,¹
LI SONG,³ AND WENXIANG CHAI^{1,*}

¹College of Materials Science and Engineering, China Jiliang University,
Hangzhou, People's Republic of China

²Jinan Cigarettes Factory, China Tobacco Shandong Industrial Co. Ltd., Jinan,
People's Republic of China

³Department of Chemistry, Key Laboratory of Advanced Textile Materials and,
Manufacturing Technology of Education Ministry, Zhejiang Sci-Tech University,
Hangzhou, People's Republic of China

Two new complexes based on the aromatic ligand [2-(4'-pyridyl)-benzoxazole] (4-PBO), Ag(4-PBO)₂NO₃ (I) and MnCl₂(4-PBO)₂(H₂O)₂ (II), are presented. Complex (I) is a wavelike supramolecular layer structure assembled by $\pi \cdots \pi$ stacking interaction, and complex (II) is a three-dimensional supramolecular framework structure assembled by $\pi \cdots \pi$ stacking and hydrogen bonding interactions. The electronic absorption and photoluminescence characterizations for complex (I) and thermal stability properties for both complexes have also been studied on as-synthesized powder samples.

Keywords Benzoxazole-pyridine ligand; crystal structure; electronic absorption spectrum; photoluminescence; supramolecule; thermal stability

Introduction

Self-assembled coordination supramolecular systems and metal-organic framework through the deliberate selection of metal ions and multifunctional ligands have received considerable recent attention. Such materials not only have potential applications as sensors, in gas storage and catalysis, or as optoelectronic and magnetic materials but also exhibit structural and topological novelty with diverse and intriguing structural motifs [1–3]. To achieve predictable combination of structural features, however, remains a great challenge [4, 5]. On the efforts to pursue the synthetic strategies for supramolecular framework, some noncovalent interactions have been emphasized repeatedly, such as hydrogen bonding, $\pi \cdots \pi$ stacking, anion $\cdots\pi$, and C-H $\cdots\pi$ interactions. These secondary interactions may be very important for different aspects such as molecular recognition and catalysis and, more specifically, for enantioselective processes [6, 7].

*Address correspondence to Wenxiang Chai, College of Materials Science and Engineering, China Jiliang University, Hangzhou 310018, People's Republic of China. E-mail: wxchai@cjlu.edu.cn.

The ligands containing 2-substituted benzimidazoles/benzoxazoles have attracted considerable interest for their antiviral activities [8], luminescent properties [9, 10], versatile coordination modes [8], and potential to form supramolecular aggregates through $\pi \cdots \pi$ stacking interactions [10, 11]. In this paper, an aromatic benzoxazole-containing pyridine ligand 2-(4'-pyridyl)-benzoxazole (4-PBO) was selected for assembling supramolecular organization, and 2 two-/three-dimensional supramolecular compounds, Ag(4-PBO)₂NO₃ (**I**) and MnCl₂(4-PBO)₂(H₂O)₂ (**II**), have been synthesized and characterized. We report herein the crystal structures and thermal stability properties of both complexes, and electronic absorption and photoluminescent (PL) properties of complex (**I**).

Experimental

Materials and General Methods

All the reagents were purchased commercially and employed without further purification. Infrared spectra were measured with a Bruker Tensor27 FT-IR spectrophotometer in the range 4000–400 cm⁻¹ in KBr lamella. Elemental analyses for C, H, and N were performed on an Elementar Vario MICRO analytic instrument. The UV-Vis and fluorescence spectral measurements were performed on Shimadzu UV3600 and Horiba Jobin-Yvon FL3-211-P spectrometers at room temperature, respectively. Thermogravimetric-differential scanning calorimetry (TG-DSC) curves were obtained in a static high purity argon atmosphere with a Mettler Toledo Simultaneous Thermal Analyzer at a heating rate of 10 K/min.

Synthesis

The complex (**I**) was synthesized by a successive-assembly reaction with mixed solvents. 0.1 mmol AgNO₃ was dissolved in 5 mL water under stirring at room temperature. And then, 10 mL ethanol solution containing 0.2 mmol 4-PBO was added to the above solution dropwise under stirring. The mixture solution was stirred at room temperature for additional half an hour. The resulting colorless solution was filtered and stayed in air. After several days, a mount of colorless block crystals were obtained, yield 87%. IR(cm⁻¹): 3114(m), 2923(w), 1653(ms), 1618(s), 1559(m), 1384(s), 1058(m), 930(m), 811(ms), 668(m), 514(m). Anal. Calc. for C₂₄H₁₆AgN₅O₅: C, 52.27; H, 2.87; N, 12.46. Found: C, 52.53; H, 2.54; N, 12.31%. The complex (**II**) was synthesized using similar method as complex (**I**) except 0.1 mmol MnCl₂·4H₂O was used. And the products in this case are a mount of yellow needle crystals, yield 82%. IR(cm⁻¹): 3413(s), 3067(w), 2922(w), 1653(m), 1618(s), 1559(m), 1541(ms), 1420(ms), 1350(ms), 1226(m), 1060(m), 1010(m), 813(m), 752(m), 700(m), 600(m), 510(m). Anal. Calc. for C₄₈H₄₀Cl₄Mn₂N₈O₈: C, 52.01; H, 3.64; N, 10.11. Found: C, 52.47; H, 3.16; N, 10.61%.

Crystal Structure Determination

Diffraction intensities for complexes **I** and **II** were collected at 293 K on an Oxford Xcalibur (Atlas Gemini ultra) diffractometer with the ω -scan technique. The structures were solved with the direct method and refined with full-matrix least squares using the SHELX package [12]. Anisotropic displacement parameters (ADPs) were applied to all non-hydrogen atoms. All H atoms bounded to C atoms were added at calculated positions and refined using a riding model, with C–H = 0.93–0.97 Å and $U_{\text{eq}}(\text{H}) = 1.2U_{\text{eq}}(\text{C})$.

Table 1. Crystal Data and Structures Refinement for **I** and **II**

| Compound\Parameter | I | II |
|---|---|---|
| Empirical formula | C ₂₄ H ₁₆ AgN ₅ O ₅ | C ₄₈ H ₄₀ Cl ₄ Mn ₂ N ₈ O ₈ |
| Color and Habit | colorless block | Yellow needle |
| Crystal size (mm) | 0.31 × 0.26 × 0.2 | 0.47 × 0.2 × 0.11 |
| Crystal system | Monoclinic | Triclinic |
| Space group | <i>P</i> 2 ₁ / <i>c</i> | <i>P</i> -1 |
| <i>a</i> (Å) | 24.179(5) | 6.4210(13) |
| <i>b</i> (Å) | 7.0946 (14) | 12.855 (3) |
| <i>c</i> (Å) | 12.735 (3) | 14.633 (3) |
| Alpha (deg.) | 90 | 106.45 (3) |
| Beta (deg.) | 92.21 (3) | 97.18 (3) |
| Gamma (deg.) | 90 | 90.09 (3) |
| Volume (Å ³) | 2182.9 (7) | 1148.4 (5) |
| <i>Z</i> | 4 | 1 |
| Formula weight | 562.29 | 1108.56 |
| Density (cal.) (mg/m ³) | 1.711 | 1.603 |
| Absorption coefficient (mm ⁻¹) | 0.972 | 0.849 |
| <i>F</i> (000) | 1128.0 | 566.0 |
| Parameter/restraints/data (obs.) | 316/15/4061 | 321/0/5032 |
| Final <i>R</i> indices (obs.) | <i>R</i> ₁ = 0.0321, <i>wR</i> ₂ = 0.0799 | <i>R</i> ₁ = 0.0422, <i>wR</i> ₂ = 0.1174 |
| <i>R</i> indices (all) | <i>R</i> ₁ = 0.0476, <i>wR</i> ₂ = 0.0954 | <i>R</i> ₁ = 0.0622, <i>wR</i> ₂ = 0.1314 |
| Goodness-of-fit | 1.157 | 1.115 |
| Largest and mean delta/sigma | 0.001, 0.000 | 0.000, 0.000 |
| Largest difference peak (e. Å ⁻³) | 0.50/−0.59 | 0.62/−0.44 |

All H atoms bounded to O atoms of water were added at calculated positions and refined using a riding model, with O—H = 0.93–0.97 Å and $U_{\text{iso}}(\text{H}) = 1.5U_{\text{eq}}(\text{O})$. In the structure **I**, the displacement parameters indicated the presence of disorder, but a split-site model combined with restraints to the ADPs did not improve the model. We therefore adopted some rigid bond restraints applied to the ADPs (DELU and SIMU parameters of 0.001 Å²). The crystal data and structure refinement details for two complexes are listed in Table 1. Selected bond lengths and angles of the complexes are collected in Table 2, and possible hydrogen bond geometries are given in Table 3.

Results and Discussion

The structure of (**I**) has been characterized as a wavelike supramolecular layer structure, in which each Ag(I) center exhibits a very distorted triangle configuration constructed by

Table 2. Selected bond lengths (Å) and angles (°) for **I** and **II**

| Compound I | | | |
|--------------------------|------------|---------------------------------------|------------|
| Ag1—O3 | 2.567(3) | Ag1—N1 | 2.222(3) |
| Ag1—N3 | 2.211(3) | | |
| N1—Ag1—O3 | 88.81(10) | N3—Ag1—O3 | 119.28(10) |
| N3—Ag1—N1 | 148.86(10) | | |
| Compound II | | | |
| Mn1—Cl1 ⁱⁱ | 2.5129(11) | Mn2—Cl2 ⁱ | 2.5257(10) |
| Mn1—Cl1 | 2.5129(10) | Mn2—Cl2 | 2.5257(10) |
| Mn1—O1 ⁱⁱ | 2.2601(19) | Mn2—O2 | 2.2589(19) |
| Mn1—O1 | 2.2601(19) | Mn2—O2 ⁱ | 2.2589(19) |
| Mn1—N1 | 2.295(2) | Mn2—N3 ⁱ | 2.273(2) |
| Mn1—N1 ⁱⁱ | 2.295(2) | Mn2—N3 | 2.273(2) |
| O1—Mn1—Cl1 ⁱⁱ | 88.14(5) | O2—Mn2—Cl2 | 87.69(5) |
| O1—Mn1—Cl1 | 91.86(5) | O2—Mn2—Cl2 ⁱ | 92.31(5) |
| O1—Mn1—N1 ⁱⁱ | 90.45(8) | O2—Mn2—N3 | 89.28(7) |
| O1 ⁱⁱ —Mn1—N1 | 90.46(8) | O2—Mn2—N3 ⁱ | 90.72(7) |
| O1—Mn1—N1 | 89.55(8) | N3—Mn2—Cl2 ⁱ | 89.49(6) |
| N1—Mn1—Cl1 | 90.45(6) | N3—Mn2—Cl2 | 90.51(6) |
| N1—Mn1—Cl1 ⁱⁱ | 89.55(6) | N3 ⁱ —Mn2—Cl2 ⁱ | 90.50(6) |

Symmetry codes: (i) $-x+1, -y, -z$; (ii) $-x, -y+1, -z+2$.

two N atoms from two pyridine rings of two 4-PBO ligands and one O atom from a nitrate (Fig. 1).

As expected, in this case, the bond lengths of Ag–N and Ag–O all are similar to those of reported structures [13–15]; however, there is one O4 atom close to the Ag(I) center with a distance of 2.766 (5) Å. Because of this close interaction, the Ag(I) coordination is not a normal triangle but a very distorted fashion which even tend to a tetrahedral configuration. Locating on the side of O4 atom, the Ag(I) present a deviation of 0.2075 (18) Å to the plane of N1–N3–O3. It is similar to the distorted coordination in a phenanthroline–Ag(I) complex reported by Swarnabala et al. [13]. There is no obvious hydrogen bonding interaction between neighboring molecules in the crystal. Whereas several sets of strong $\pi \cdots \pi$ interactions could be found between all face-to-face ligand planes from two neighboring molecules [5, 16].

Table 3. Hydrogen-bond geometry (Å, °) for (II)

| $D\cdots H\cdots A$ | $D\cdots H$ | $H\cdots A$ | $D\cdots A$ | $D\cdots H\cdots A$ |
|------------------------------------|-------------|-------------|-------------|---------------------|
| O1—H1A \cdots Cl2 ⁱ | 0.92 | 2.34 | 3.2369(8) | 167 |
| O1—H1B \cdots Cl1 ⁱⁱ | 0.92 | 2.34 | 3.1416(7) | 146 |
| O2—H2A \cdots Cl2 ⁱⁱⁱ | 0.94 | 2.32 | 3.1410(7) | 147 |
| O2—H2B \cdots Cl1 ^{iv} | 0.94 | 2.39 | 3.2115(7) | 146 |

Symmetry codes: (i) $-x+1, -y, -z+1$; (ii) $x+1, y, z$; (iii) $-x+2, -y, -z$; and (iv) $x+1, y, z-1$.

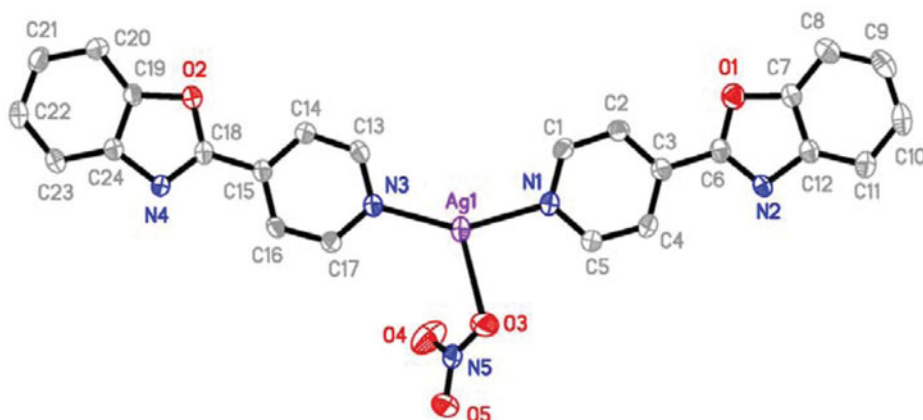


Figure 1. Molecular structure and labeling of complex (I) with displacement ellipsoids drawn at the 30% probability level.

As shown in Fig. 2, all of the face-to-face ligand planes are parallel to each other with a very short distances of interplane 3.3805 (19) Å and plane centroid to plane centroid 3.9337 (19) Å ($\pi \cdots \pi$ interaction NO. 1), interplane 3.405 (2) Å and plane centroid to plane centroid 3.6765 (19) Å ($\pi \cdots \pi$ interaction NO. 2), interplane 3.497 (2) Å and plane centroid to plane centroid 3.8078 (18) Å ($\pi \cdots \pi$ interaction NO. 3), and interplane 3.433 (2) Å and plane centroid to plane centroid 3.8398 (18) Å ($\pi \cdots \pi$ interaction NO. 4), respectively. By virtue of these strong $\pi \cdots \pi$ interactions, all of molecules fuse together and give rise to a wavelike supramolecular layer structure along the *ab* plane (Fig. 3). And as shown in Fig. 4, an alternant A-B-A-B packing model of these layers could be found along the *c*-axis.

The structure of (II) has been characterized as a three-dimensional supramolecular framework structure, in which each Mn(II) center exhibits a octahedral trans-configuration

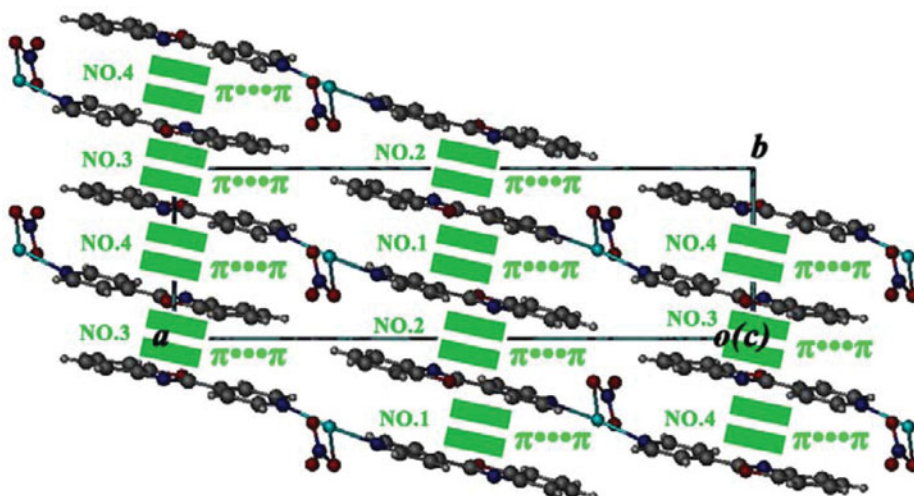


Figure 2. A wavelike supramolecular layer structure extending along the *ab* plane in (I) assembled by four sets of π - π interactions, viewed along the *c*-axis.

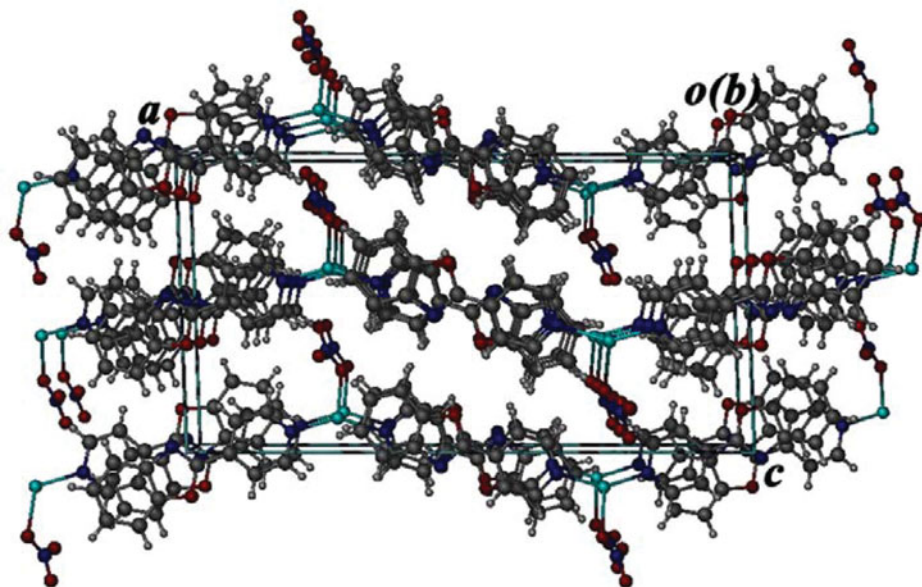


Figure 3. Wavelike supramolecular layer structures in (I) and their stacking along the c direction, viewed along the b -axis.

constructed by two N atoms from two 4-PBO ligands, two O atoms of water and two Cl atoms (Fig. 5).

This trans-configuration is similar to that of pyridine analogue [17]. And in this case, the bond lengths of Mn–N, Mn–O, and Mn–Cl all are similar to those of reported structures [17–19]. There are some weak hydrogen bonding interactions between neighboring

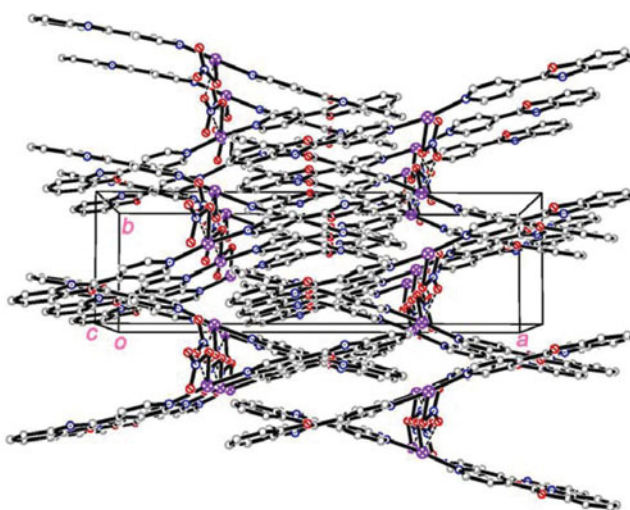


Figure 4. The A-B-A-B alternant stacking fashion of the layers in the packing diagram of (I).

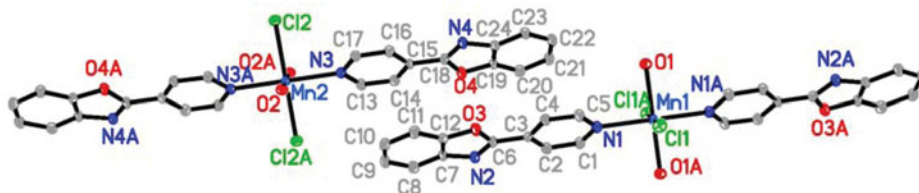


Figure 5. Molecular structure and labeling of complex (II) with displacement ellipsoids drawn at the 30% probability level.

molecules in the crystal [20] (details in Table 3). On account of these hydrogen bonding interactions, all of the molecules connect each other to form a supramolecular layer extended along the *ab* plane (Fig. 6).

And there also are some strong $\pi \cdots \pi$ interactions between all face-to-face ligand planes from two neighboring molecules [5, 16]. As shown in Fig. 7, all of the face-to-face ligand planes are parallel to each other with a very short distances of inter-plane 3.4201 (15) Å and plane centroid to plane centroid 3.7022 (15) Å ($\pi \cdots \pi$ interaction NO. 1), and interplane 3.3950 (17) Å and plane centroid to plane centroid 3.6686 (17) Å ($\pi \cdots \pi$ interaction NO. 2), respectively. By virtue of these strong $\pi \cdots \pi$ interactions, all of these supramolecular layers fuse together and present a three-dimensional supramolecular framework structure. As shown in Fig. 8, the packing of this supramolecular structure is close so that there is no any guest resided in its framework.

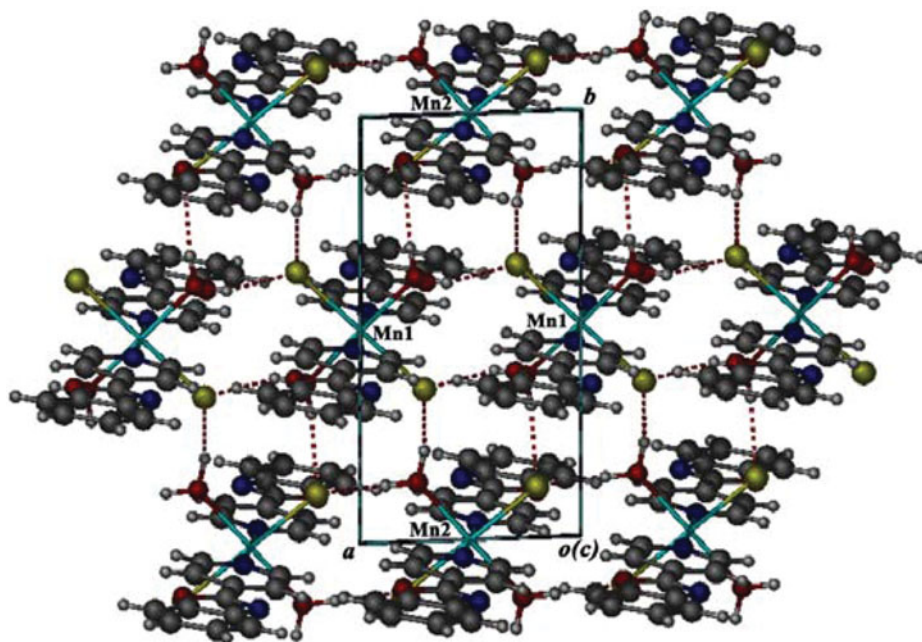


Figure 6. A supramolecular layer structure assembled by hydrogen bonding interactions extending along the *ab* plane in (II), viewed along the *c*-axis.

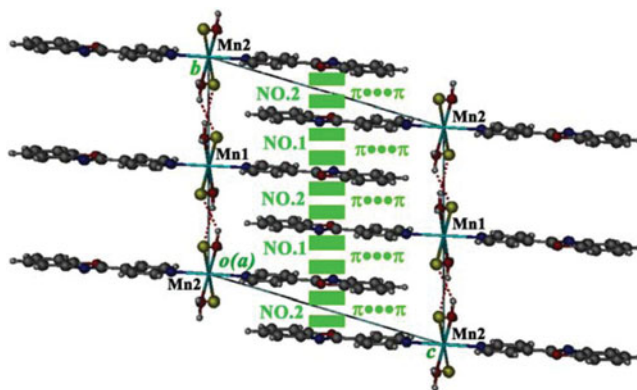


Figure 7. A three-dimensional supramolecular structure in complex (II) assembled by hydrogen bonding and two sets of π - π stacking interactions, viewed along the a -axis.

The UV-Vis diffuse reflection spectrum of complex (I) was recorded on the as-synthesized powder, and plotted in Fig. 9 as $F^2(R)$ versus wavelength, according to the Kubelka-Munk function [21, 22]. The strong high-energy absorption band peaked at ~ 350 nm should be assigned as the π - π^* transition of 4-PBO ligand, which often could be found at same region from aromatic ligands or their complexes [23]. Beyond this π - π^* transition band, a weak band centered at ~ 450 nm could be found. According to previous reports around luminescent silver(I) complexes [24], this weak absorption band should be assigned as a metal-to-ligand charge transfer MLCT transition band.

The solid-state emission and excitation spectra have also been recorded on as-synthesized powder samples for complex (I) (Fig. 10). Under an irradiation with the wavelength varying from 300 to 600 nm, the complex consistently emits red light and its PL emission spectrum is broad (the full width at half maximum, FWHM = ~ 150 nm) with the λ_{max} value at ~ 640 nm. This PL emission could be derived from some MLCT excited states or ligand centered states benefited from the spin-orbit coupling of silver [24].

For investigating the thermal stability of two complexes, the coinstantaneous thermogravimetric (TG) and DSC measurements were carried out on as-synthesized powder

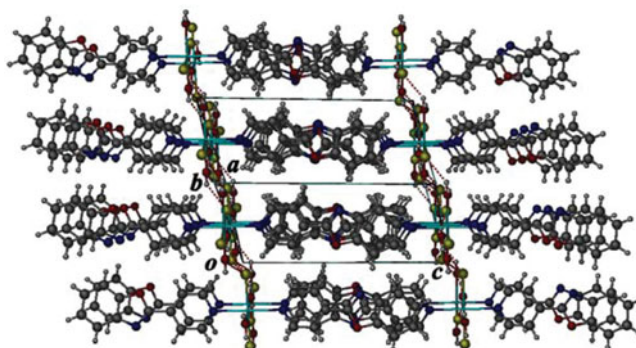


Figure 8. The packing diagram of structure (II) present a supramolecular framework structure, viewed along the $[1 -1 0]$ axis.

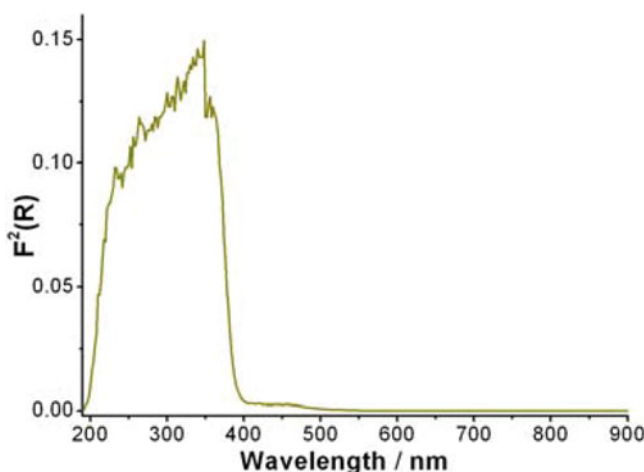


Figure 9. The UV-Vis diffuse reflection spectrum recorded on powder sample of complex (I) at room temperature.

samples. As shown in Fig. 11, complex (I) could resist decomposition until to ~ 473 K, and then undergoes a large loss-weight process from 473 to 553 K with a weight-loss of $\sim 70\%$ corresponding to the release of all ligand (calculated value 69.8%). The TG-DSC curves of complex (II) are shown in Fig. 12, in which three obvious weight-loss steps could be found. Firstly, the weight loss of $\sim 6.7\%$ in the range ~ 433 – 453 K corresponds to the release of the coordinated water molecule (calculated value 6.5%). This good resistance to decomposition should be benefit from some hydrogen bondings and the close packing of the supramolecular framework in (II). And then from ~ 543 to 603 K, the second step exhibits a large weight loss of $\sim 42\%$, following by the third step from ~ 603 to 653 K with

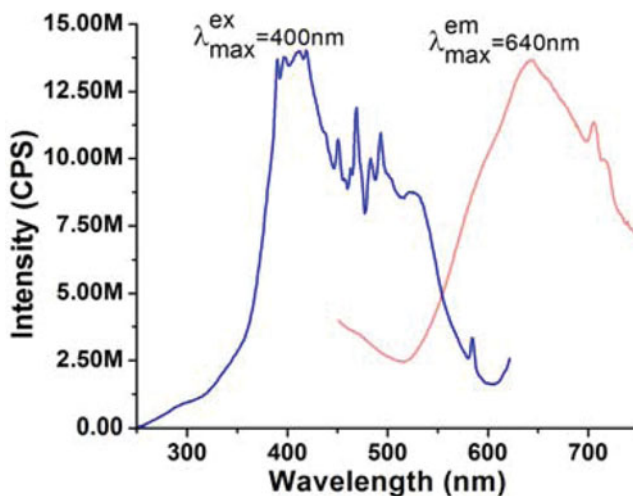


Figure 10. The photoluminescent emission (a, $\lambda_{\text{ex}} = 400$ nm) and excitation (b, $\lambda_{\text{em}} = 640$ nm) spectra recorded on powder sample of complex (I) at room temperature.

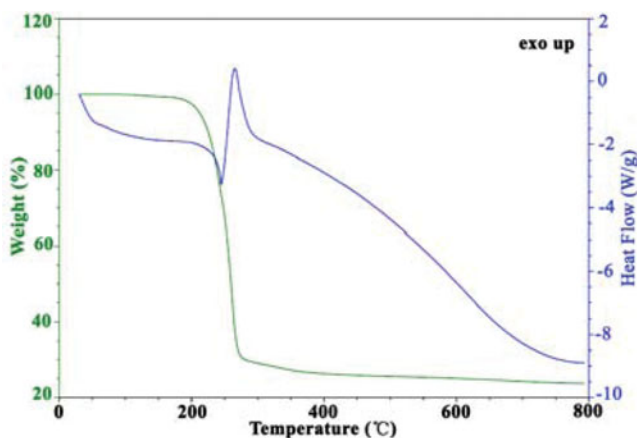


Figure 11. The TG and DSC curves of complex (I).

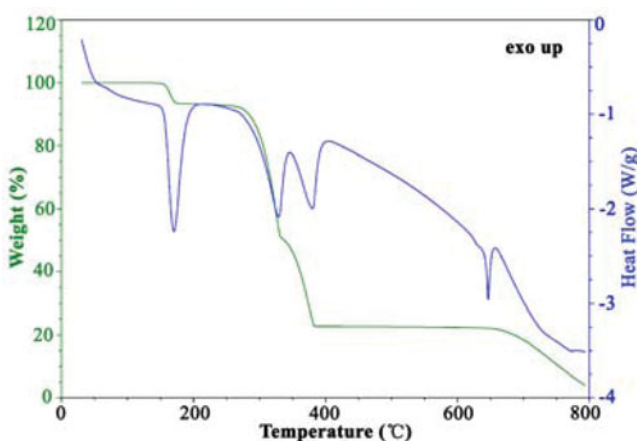


Figure 12. The TG and DSC curves of complex (II).

a weight loss of $\sim 29\%$. Both of these two steps with total weight-loss of $\sim 71\%$ should be corresponding to the release of all ligand (calculated value 70.8%), thus the residue should be MnCl_2 (observed 22.5% , calculated 22.7%). Between these two steps, an intermediate could be present with a formula as $\text{MnCl}_2(4\text{-PBO})_{0.8}$. It also could be a result caused by the strong $\pi \cdots \pi$ stacking interactions in the supramolecular framework.

Conclusion

In conclusion, the successful self-assembly of aromatic ligand 4-PBO and Ag(I) / Mn(II) lead to two novel two-/three-dimensional supramolecular structures. Both of them present good thermal stability, and the photoluminescent property of complex (I) also been observed. For searching novel structures and functions, explorations of the rational assemble of 2-substitued benzimidazoles/benzoxazoles ligands with other metallic ions, such as magnetic Co(II) and Ni(II) or luminescent Cu(I) and Zn(II), are ongoing.

Supplementary Material

Crystallographic data for the structures reported here have been deposited with CCDC (Deposition No. CCDC-1022449 (I), No. CCDC-1022450 (II)). These data can be obtained free of charge via <http://www.ccdc.cam.ac.uk/conts/retrieving.html> or from CCDC, 12 Union Road, Cambridge CB2 1EZ, UK, E-mail: deposit@ccdc.cam.ac.uk.

Acknowledgments

The authors are grateful for financial support from the National Natural Science Foundation of China (project no. 61205184, 11175169), and the Natural Science Foundation of Zhejiang Province (project no. LY12E02010).

References

- [1] Miyazaki, S., Kojima, T. & Fukuzumi, S. (2008). *J. Am. Chem. Soc.*, **130**, 1556–1557.
- [2] Badjica, J. D., Nelson, A., Cantrill, S. J., Turnbull, W. B. & Stoddart, J. F. (2005). *Acc. Chem. Res.*, **38**, 723–732.
- [3] Ockwig, N. W., Delgado-Friedrichs, O., O’Keeffe, M. & Yagi, O. M. (2005). *Acc. Chem. Res.*, **38**, 176–182.
- [4] Kim, J. H., *et al.* (2001). *J. Am. Chem. Soc.*, **123**, 8239–8247.
- [5] Chai, W.-X., *et al.* (2012). *J. Inorg. Organomet. Polym.*, **22**, 1263–1270.
- [6] Yoshizawa, M., Tamura, M. & Fujita, M. (2006). *Science*, **312**, 251–254.
- [7] Braga, D., Grepioni, F. & Desiraju, G. R. (1998). *Chem. Rev.*, **98**, 1375–1405.
- [8] Tidwell, R. R., *et al.* (1993). *Antimicrob. Agents Chemother.*, **37**, 1713–1716.
- [9] Gao, L.-H., Guan, M., Wang, K.-Z., Jin, L.-P., & Huang, C.-H. (2006). *Eur. J. Inorg. Chem.*, 3731–3737.
- [10] Tong, Y.-P., Zheng, S.-L. & Chen, X.-M. (2005). *Inorg. Chem.*, **44**, 4270–4275.
- [11] Moon, D., Lah, M. S., Sesto, R. E. D. & Miller, J. S. (2002). *Inorg. Chem.*, **41**, 4708–4714.
- [12] Sheldrick, G. M. (2008). *Acta Cryst.*, **A64**, 112–122.
- [13] Swarnabala, G. & Rajasekharan, M. V. (1996). *Polyhedron*, **15**, 3197–3201.
- [14] Sailaja, S., Swarnabala, G. & Rajasekharan, M. V. (2001). *Acta Cryst.*, **C57**, 1162–1165.
- [15] Yue, N. L. S., Jennings, M. C. & Puddephatt, R. J. (2005). *Inorg. Chem.*, **44**, 1125–1131.
- [16] Chai, W.-X., *et al.* (2012). *Solid State Sci.*, **14**, 1226–1232.
- [17] Kathikeyan, M., Kathikeyan, S. & Manimaran, B. (2011). *Acta Cryst.* **E67**, m1367–m1368.
- [18] Goher, M. A. S., Abu-Youssef, M. A. M., Mautner, F. A. & Popitsch, A. (1993). *Polyhedron*, **12**, 1751–1756.
- [19] Luneau, D., *et al.* (1993). *Inorg. Chem.*, **32**, 5616–5622.
- [20] Chai, W.-X., *et al.* (2010). *Solid State Sci.*, **12**, 2100–2105.
- [21] Chai, W.-X., Wu, L.-M., Li, J.-Q. & Chen, L. (2007a). *Inorg. Chem.*, **46**, 1042–1044.
- [22] Chai, W.-X., Wu, L.-M., Li, J.-Q. & Chen, L. (2007b). *Inorg. Chem.*, **46**, 8698–8704.
- [23] Hong, M.-W., *et al.* (2014). *J. Cluster Sci.*, DOI: 10.1007/s10876-014-0762-9 (Published online).
- [24] Hsu, C. W., *et al.* (2011). *J. Am. Chem. Soc.*, **133**, 12085–12099.